Bol. Soc. Paran. Mat.
©SPM – E-ISSN-2175-1188
SPM: www.spm.uem.br/bspm

(3s.) **v. 2026 (44) 17** : 1–19.
ISSN-0037-8712
doi:10.5269/bspm.82351

Numerical Investigation of Joule Heating and Suction Effects on MHD Casson Nanofluid Flow over Exponential Stretching Sheet with Thermal Radiation and Chemical Reaction

Kethoju Chandana, S. Hari Singh Naik and Ramesh Kune

ABSTRACT: The main part of the current examination is to forecast the consequence of the simultaneous incorporation of joule heating, radiation absorption with chemical reaction on Casson fluid flow across an exponentially stretching surface under the influence of various flow parameters. The resulting partial differential equations are transitioned into ordinary differential equations by employing a suitable similarity transformation. The resultant equations are computed numerically using MATLAB bvp4c built-in technique. In order to justify the precision of the numerical method used, the numerical values obtained in a constrained scenario are correlated with the outcomes existing in the literature. The impacts of multifarious dimensionless parameters on velocity profile, temperature and concentration distributions are illustrated graphically. The effect of involved parameters on skin friction coefficient, Nusselt number and Sherwood number are tabulated. The findings are evaluated for essential industrial and technical characteristics such as Nusselt numbers, temperatures, skin frictions, and velocity. The Combined influence of joule heating ,radiation absorption with the incorporation of an exponential parameter on the flow field is trailblazing since joule heating and the radiation absorption skyrockets the temperature, but on the contrary, chemical reaction depreciates the temperature.

Keywords: Casson fluid, Joule heating parameter, Suctions parameter, Chemical reaction and Radiation parameter.

Contents

1 Introduction 1

2 Mathematical Formulation 3

3 Method of Solution 4

4 Numerical Procedure 5

5 Results and Discussions 6

6 Conclusion 17

1. Introduction

The transport phenomena associated with boundary-layer flow over stretched surfaces continue to play a prominent role in fluid mechanics and applied mathematics due to their wide range of applications in processes such as continuous casting, glass fiber drawing, polymer extrusion, and cooling metallic plates. Stretching-sheet idealizations, which are theoretically tractable yet physically meaningful due to the imposed surface motion creating substantial velocity and heat gradients in the neighboring fluid region, are commonly used to depict these industrial systems [1,2]. One essential component of modern fluid dynamics research is the study of boundary layer transport on stretching surfaces. According to the ground-breaking research of [1], industrial sheet drawing processes where stretching velocity, temperature, and concentration fluctuate nonlinearly along the surface can be more realistically depicted by exponentially stretching surfaces.

Early research primarily assumed linear stretching velocities, but it has been shown that many real-world manufacturing processes show spatially variable stretching rates, which exponential stretching laws better capture. In 1999, [1] established similarity solutions for exponentially stretching sheets and showed that, in contrast to power-law or linear stretching models, exponential stretching significantly changes the structure of the velocity and temperature fields. Later research that included wall mass transfer

2020 *Mathematics Subject Classification:* 76W05, 76D10, 80A20.
Submitted March 03, 2026. Published June 19, 2026.

by injection or suction shown that suction improves boundary-layer stability and increases heat transfer rates, offering an extra thermal control mechanism [3].

The introduction of Lorentz forces by a magnetic field in electrically conducting fluids resists fluid motion and dramatically alters momentum and heat transport properties. Due to its uses in metallurgical processing, nuclear reactor cooling, electromagnetic flow control, and MHD generators, this magnetohydrodynamic (MHD) phenomenon has garnered ongoing research [4,5] It has been demonstrated that adding MHD effects to exponentially stretched sheet models suppresses velocity profiles while increasing temperature distributions because of resistive heating and decreased convective transport [6,7].

Many biological and industrial fluids have non-linear rheological behavior and yield stress that go beyond Newtonian fluid assumptions and are not well represented by traditional viscous models. Originally developed for pigment-oil suspensions, the Casson fluid model has become a commonly used approximation for yield-stress fluids, including blood, printing inks, honey, and polymeric melts [8].Numerous authors have studied Casson fluid flow over exponentially extending permeable surfaces and found that the Casson parameter has a significant impact on heat transfer rates, boundary-layer thickness, and shear stress [9,10].

In high-temperature processes and optically involved mediums, where radiative heat flux dramatically changes the energy balance, thermal radiation takes over as the primary heat transfer mechanism. It has been shown that adding thermal radiation to stretching-sheet models significantly increases temperature fields and decreases surface heat transfer rates [11,12].

By transforming incident radiation into thermal energy, radiation absorption in radiative environments intensifies thermal boundary layers and adds to internal energy creation [13]. The combined effects of chemical reaction and radiation absorption have been investigated in a variety of flow configurations, such as accelerating surfaces, porous media, and oscillatory plates. Radiation absorption raises temperatures, according to these research, but chemical reactions tend to lower concentrations and, in certain situations, inhibit thermal transport [14,15,16].

Such investigations were more recently extended to complicated rheological and nanofluid systems by [17,18], highlighting the increasing significance of multi-physical coupling in contemporary transport models. The sensitivity of temperature profiles to radiative factors was highlighted by [19] in their study of Casson fluid flow with radiation absorption and slip effects on stretching surfaces. [20] examined MHD Casson flows with heat generation and chemical reactions, emphasizing the interplay between concentration and thermal fields. In their investigation of the effects of radiation and viscous dissipation in MHD stretching flows, [21] verified a notable thickening of the thermal boundary layer. These models were subsequently expanded by [22] and [23] by incorporating internal heating, slide, and suction mechanisms in Casson MHD topologies.

A thorough analysis of each of the aforementioned investigations reveals a noteworthy and recurring finding. In each study, the Lorentz force has been used as a resistive mechanism to bring the magnetic field into the momentum equation. But according to basic MHD theory, electric currents are created when a fluid that conducts electricity travels in a magnetic field. Joule (Ohmic) heating, which is formally represented by $\sigma B^2 u^2$, is the internal heat produced by these currents as a result of electrical resistance [24,25]. The direct transformation of electromagnetic energy into thermal energy is referred to by this phrase. Despite its basic significance, prior research on Casson fluid flow across exponentially stretched sheets with radiation absorption and chemical reaction has not included this Joule heating contribution in the energy equation.

Since Casson rheology modifies velocity gradients because of yield stress, exponential stretching increases the velocity magnitude along the sheet, and large magnetic fields create significant electrical currents, this omission becomes very important. It is therefore anticipated that in such flows, Joule heating will function as the primary internal heat generating mechanism. Inspired by these findings, the current study builds on the research of [26] by adding a Joule heating-type contribution to the temperature governing equation.

The current formulation offers a more energetically complete explanation of MHD Casson fluid transport over an exponentially stretched sheet than previous studies that took into account radiation absorption and chemical reaction without electromagnetic heating.

In accordance with exponential stretching velocity, temperature, and concentration distributions,

the controlling partial differential equations are converted into a coupled system of nonlinear ordinary differential equations by applying the proper similarity transformations and are solved numerically by MATLAB bvp4c solver. The accuracy of the current calculations is verified by comparing them with the benchmark findings for limiting scenarios that are currently available. The resulting boundary-value issue is then solved numerically using a proven finite-difference scheme. In order to provide a deeper understanding of thermal control mechanisms pertinent to advanced manufacturing and MHD-based thermal systems, the results of this investigation are anticipated to enhance the body of existing literature by clarifying the synergistic interaction of Casson rheology, magnetic field, radiation absorption, chemical reaction, and Joule heating.

2. Mathematical Formulation

An incompressible, electrically conducting Casson fluid flowing steadily in two dimensions across an exponentially stretched surface is taken into consideration. The y-axis is assumed to be normal to the surface, and the origin O is fixed on the sheet that extends along the x-direction. The fluid motion is restricted to the region $y > 0$,and the sheet is assumed to coincide with the plane $y = 0$. A transverse magnetic field of varying strength is applied normal to the surface, expressed as $B(x) = B_0 e^{\frac{N.x}{2L}}$ where B_0 indicates the constant strength of the reference magnetic field, N stands for the exponential stretching parameter, and L is the sheet's characteristic length. Figure. 1 shows a schematic representation of the coordinate system and physical configuration that correspond to these assumptions.

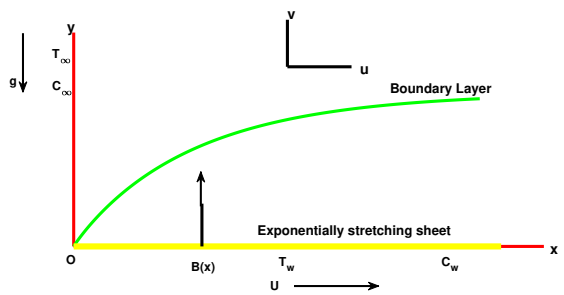

Figure 1: An illustration of the fluid flow problem.

$$\frac{\partial u}{\partial x} + \frac{\partial v}{\partial y} = 0 \tag{2.1}$$

$$u\frac{\partial u}{\partial x} + v\frac{\partial u}{\partial y} = \nu\left(1 + \frac{1}{\beta}\right)\frac{\partial^2 u}{\partial y^2} + g\beta_T(T - T_\infty) + g\beta_C(C - C_\infty) - \frac{\sigma B^2}{\rho}u \tag{2.2}$$

$$\rho c_P\left(u\frac{\partial T}{\partial x} + v\frac{\partial T}{\partial y}\right) = \kappa\frac{\partial^2 T}{\partial y^2} - \frac{\partial q_r}{\partial y} + \mu_B\left(1 + \frac{1}{\beta}\right)\left(\frac{\partial u}{\partial y}\right)^2 + Q(T - T_\infty) + Q^*(C - C_\infty) + \sigma B^2 u^2 \tag{2.3}$$

$$u\frac{\partial C}{\partial x} + v\frac{\partial C}{\partial y} = D_m\frac{\partial^2 C}{\partial y^2} - k_l(C - C_\infty) \tag{2.4}$$

The symbols u and v stand for the velocity components along the x- and y-directions, respectively. ν is a representation of the fluid's kinematic viscosity. The expression for the Casson fluid parameter is

$$\beta = \frac{\mu_B\sqrt{2\pi_c}}{p_y}.$$

where μ_B is the plastic dynamic viscosity and p_y is the yield stress of the fluid. The fluid temperature and concentration are indicated by the numbers T and C, whilst the ambient temperature and concentration

are indicated by the numbers T_∞ and C_∞, respectively. The symbols σ, ρ, ρc_P, κ, and D_m stand for electrical conductivity, density, heat capacitance, thermal conductivity, and mass diffusivity. The equations for the chemical process, radiation absorption, and heat source that vary exponentially on space are as follows:

$$Q = Q_0 e^{Nx/L}, \qquad k_l = k_0 e^{Nx/L}, \qquad Q^* = Q_0^* e^{Nx/L}.$$

Rosseland diffusion approximation is used to represent heat radiation in an optically thick medium [13]. Consequently, the radiative heat flux is provided by

$$q_r = -\frac{4\sigma^*}{3k^*}\frac{\partial T^4}{\partial y}.$$

where σ^* represents the Stefan–Boltzmann constant and k^* represents the mean absorption coefficient. When higher-order terms are ignored and T^4 is extended in a Taylor series around the ambient temperature T_∞, assuming that the temperature changes within the boundary layer are minimal, the result is

$$T^4 \approx 4T_\infty^3 T - 3T_\infty^4.$$

.

The radiative heat term is simplified when this approximation is substituted into the energy equation(2.3), and the energy equation becomes

$$\rho c_P \left(u\frac{\partial T}{\partial x} + v\frac{\partial T}{\partial y}\right) = \kappa\left(1 + \frac{16\sigma^* T_\infty^3}{3\kappa k^*}\right)\frac{\partial^2 T}{\partial y^2} + \mu_B\left(1+\frac{1}{\beta}\right)\left(\frac{\partial u}{\partial y}\right)^2 + Q(T-T_\infty) + Q^*(C-C_\infty) + \sigma B^2 u^2. \tag{2.5}$$

The boundary conditions are

$$\text{at } y = 0, \quad u = U,\ v = -V(x),\ T = T_w,\ C = C_w. \tag{2.6}$$

$$\text{as } y \to \infty, \quad u \to 0,\ T \to T_\infty,\ C \to C_\infty. \tag{2.7}$$

Assuming exponential variation along the surface at this point, the sheet's stretching velocity is determined by $U = U_0 e^{Nx/L}$,where L is the characteristic length and U_0 is the reference stretching velocity. Additionally, it is assumed that the surface temperature and concentration change exponentially along the sheet, and they are described as

$$T_w = T_\infty + T_0 e^{Nx/2L}, \qquad C_w = C_\infty + C_0 e^{Nx/2L},$$

where T_0 and C_0 represents the reference temperature and reference concentration, respectively. The normal velocity at the wall is taken in the exponential form

$$V(x) = V_0 e^{Nx/2L}$$

where V_0 is a constant. The condition $V(x) > 0$ represents suction at the surface, while $V(x) < 0$ corresponds to blowing (injection) of the fluid through the sheet.

3. Method of Solution

Using the following Similarity Transformations

$$\eta = \sqrt{\frac{U_0}{2\nu L}}\, e^{\frac{Nx}{2L}}\, y. \tag{3.1}$$

$$u = U_0 e^{Nx/L} f'(\eta). \tag{3.2}$$

$$v = -\sqrt{\frac{\nu U_0}{2L}}\, e^{\frac{Nx}{2L}} N\left[f(\eta) + \eta f'(\eta)\right]. \tag{3.3}$$

$$T = T_\infty + T_0 e^{\frac{Nx}{2L}}\, \theta(\eta). \tag{3.4}$$

$$C = C_\infty + C_0 e^{\frac{Nx}{2L}}\,\phi(\eta). \tag{3.5}$$

When Eqs.(3.1) to (3.5) are substituted in Eqs.(2.2), (2.5) and (2.4), the governing equations change to the coupled ODEs shown below

$$\left(1+\frac{1}{\beta}\right) f''' + N\left(ff'' - 2\left(f'\right)^2\right) + 2Gr\,\theta + 2Gc\,\phi - Mf' = 0. \tag{3.6}$$

$$\frac{1}{Pr}\left(1+\frac{4}{3}R\right)\theta'' - N\left(f'\theta - f\theta'\right) + Ec\left(1+\frac{1}{\beta}\right)\left(f''\right)^2 + Q_H\theta + R_a\phi + Jh\left(f'\right)^2 = 0. \tag{3.7}$$

$$\phi'' - N\,Sc\left(f'\phi - f\phi'\right) - 2k\,Sc\,\phi = 0. \tag{3.8}$$

Likewise, using Eqs.(3.1) to (3.5) in Eqs.(2.6)and (2.7) results in

$$f(0) = S, \quad f'(0) = 1, \quad \theta(0) = 1, \quad \phi(0) = 1. \tag{3.9}$$

$$f'(\eta) \to 0, \quad \theta(\eta) \to 0, \quad \phi(\eta) \to 0 \quad \text{as } \eta \to \infty. \tag{3.10}$$

Where η is the variable of similarity,$f(\eta)$ is the dimensionless stream function,$\theta(\eta)$ is the dimensionless temperature, $\phi(\eta)$ is the dimensionless concentration and prime indicates the differentiation w.r.to η, $Gr = \dfrac{gL\beta_T(T_w - T_\infty)}{U^2}$ is Thermal Grashof number, $Gc = \dfrac{gL\beta_C(C_w - C_\infty)}{U^2}$ is solutal Grashof number, $M = \dfrac{2L\sigma B_0^2}{\rho U_0}$ is the Magnetic field parameter, $Pr = \dfrac{\nu}{\alpha}$ denoted Prandtl number where α is thermal diffusivity, $R = \dfrac{4\sigma^* T_\infty^3}{kk^*}$ is Radiation Parameter, $Ec = \dfrac{U^2}{c_P\left(T_w - T_\infty\right)}$ is Eckert number, $Q_H = \dfrac{2Q_0 L}{U_0\rho c_P}$ is Heat source/sink, $R_a = \dfrac{2Q_0^* C_0 L}{U_0 T_0 \rho c_P}$ is Radiation absorption parameter, $Jh = M\,Ec$ is Joules heating parameter,$Sc = \dfrac{\nu}{D_m}$ is Schmidt number,$k = \dfrac{k_0 L}{U_0}$ is the Chemical reaction parameter and $S = \dfrac{v_0}{\sqrt{\dfrac{\nu U_0}{2L}}}$ is suction/injection. The skin-friction coefficient C_f, local Nusselt number Nu_x, and local Sherwood number Sh_x are defined as

$$\frac{C_f\sqrt{Re_x/2}}{\sqrt{x/L}} = \left(1+\frac{1}{\beta}\right) f''(0),$$
$$\frac{Nu_x}{\sqrt{Re_x/2}\,\sqrt{x/L}} = -\theta'(0),$$
$$\frac{Sh_x}{\sqrt{Re_x/2}\,\sqrt{x/L}} = -\phi'(0).$$

where the local Reynolds number is defined as $Re_x = \dfrac{Ux}{\nu}$. The shear stress, heat transfer rate, and mass transfer rate at the stretched surface are calculated using these formulas based on the numerical solutions.

4. Numerical Procedure

For the purpose of solving boundary value problems, MATLAB provides a framework. The MATLAB package called bvp4c [27], a finite difference approach that includes the three-stage Lobatto IIIa collocation formula, is used to solve the transmogrified equations numerically.The BVP can be changed as an initial value problem (IVP) to affect bvp4c [28].We change the modified system of Eqs.(3.6) to (3.10) into a first-order system by introducing new variables as follows

$$y_1 = f, \quad y_2 = f', \quad y_3 = f'', \quad y_4 = \theta, \quad y_5 = \theta', \quad y_6 = \phi, \quad y_7 = \phi'.$$

$$y_3' = \frac{1}{(1+\frac{1}{\beta})}\left[-N\left(y_1y_3 - 2y_2^2\right) - 2Gr\, y_4 - 2Gc\, y_6 + My_2\right]$$

$$y_5' = \frac{Pr}{(1+\frac{4}{3}R)}\left[N\left(y_2y_4 - y_1y_5\right) - Ec\left(1+\frac{1}{\beta}\right)y_3^2 - Q_H y_4 - R_a y_6 - Jh\, y_2^2\right]$$

$$y_7' = N\, Sc\left(y_2y_6 - y_1y_7\right) + 2k\, Sc\, y_6$$

with the boundary conditions

$$y_1(0) = S, \quad y_2(0) = 1, \quad y_4(0) = 1, \quad y_6(0) = 1, y_2(\infty) \to 0, \quad y_4(\infty) \to 0, \quad y_6(\infty) \to 0$$

Through mesh adaptation and error control, the bvp4c method iteratively refines the solution, treating the boundary value problem similarly to an initial value problem. This approach is put into practice by first transforming the higher-order differential equations into a system of first-order equations. For the unknown boundary values, appropriate beginning assumptions are then provided in order to start the iterative process. The asymptotic boundary conditions are sufficiently represented by the finite value $\eta_{\max} = 10$, which truncates the computational domain.

5. Results and Discussions

For the Newtonian fluid under particular limiting circumstances, the numerical values of $f''(0)$ and $-\theta'(0)$ are compared with results that have already been published in the literature. The current results are found to be in excellent agreement with those reported by Mukhopadhyay et al. [9], Bidin and Nazar [12], Elbashbeshy [3], and Magyari and Keller [1] ,Nandhini et al [26] for the case where the exponential parameter is unity and mass transfer, magnetic field, heat source/sink, buoyancy effects, buoyancy effects, and suction/injection are not present. Table 1. Describes the comparison between previous and present out comes. According to the Table 2. Skin friction value increases (for R=0) with escalation in Pr. & decrease with the increasing values of R .Table 3.Shows the variation in coefficient of skin friction ,Nusselt and Sherwood values with the different parameter.

Table 1: Correlation of $f''(0)$ under special case for Newtonian fluid

Magyari and Keller [1]	Elbashbeshy [3]	Bidin and Nazar [12]	Mukhopadhyay et al [9].	Nandhini et al. [26]	Present study
−1.28180	−1.28181	−1.28180	−1.28182	−1.28182	−1.28182

Table 2: Correlation of $-\theta'(0)$ for variation in Pr and R for Newtonian fluid

Pr	**R**	**Nandhini et al. [26]**	**Present study with $N = 1$**
1	0	0.9548	0.9548
2	0	1.4715	1.4715
3	0	1.8691	1.8691
5	0	2.5001	2.5001
10	0	3.6603	3.6603
1	0.5	0.6767	0.6767
1	1	0.5313	0.5313
2	0.5	1.0735	1.0735
2	1	0.8629	0.8629
3	0.5	1.3807	1.3807
3	1	1.1214	1.1214

The process is introduced to examine the coupled result of fluid flow equation during the transitory MHD Casson flow moving across a exponential stretching surface. The equations intended for velocity $f'(\eta)$, temperature θ, and concentration ϕ are approved through bvp4c. For the numerical analysis of this study, the numbers $M = 0.5$, $R_a = 0.5$, $Gr = Gc = 1$, $Pr = 0.71$, $Sc = 0.6$, $S = 0.5$, $N = 0.5$,

Table 3: Tabulation of numerical values of $(1+\frac{1}{\beta})f''(0)$, $-\theta'(0)$ and $-\phi'(0)$ for Casson fluid with fixed values of $Pr = 0.7$, $Sc = 0.6$ and $S = 0$.

M	R	N	k	Q_H	E_c	R_a	Gr	Gc	$(1+\frac{1}{\beta})f''(0)$	$-\theta'(0)$	$-\phi'(0)$
0.5	0.3	1	0.1	0.4	0.01	0.5	1	1	-0.6384	0.6417	1.1345
0.8									-0.8266	0.6223	1.1259
1.2									-1.0639	0.5974	1.1151
0.5	0.5								-0.5792	0.5781	1.1392
	0.8								-0.5069	0.5089	1.1450
	0.3	2							-2.3296	1.1535	1.6131
		3							-3.5481	1.5653	2.0385
		0.5	0.3						0.4479	1.5653	2.0385
			0.5						0.3738	0.3428	1.0990
			0.1	0.6					0.7000	0.2032	0.8376
				0.8					0.8919	0.0424	0.8497
				0.4	0.05				0.5726	0.3015	0.8270
					0.1				0.6835	0.2183	0.8194
					0.01	0.7			-2.1330	0.8536	0.7334
						0.9			0.9014	0.1162	0.8537
						0.5	3		3.2857	0.4073	0.9130
							5		5.3183	0.4715	0.9462
							1	3	2.5151	0.4405	0.8729
								5	4.3550	0.5204	0.9105

$R = 0.3$, $Q_H = 0.4$, $\beta = 0.5$, and $k = 0.1$ are all considered constants. Any deviations from these data are clearly noted in the relevant figures.

Figure 2.Demonstrates the prevalence of M on $f'(\eta)$. For $N = 1$, amelioration of M depreciates $f'(\eta)$. The movement of fluid transport rate is notably deteriorating asa repercussion of the transverse magnetic field, which foment drag force. This force is induced in terms of Lorentz force,which works in the opposite direction to the fluid motion. Moreover, Lorentz force escalates as M augments, which in-turn resists the flow to a greater extent. Moreover, soaring the values of, increases the thermal and solutal boundary layer thickness. On the other hand of this, $\theta(\eta)$ and η gets escalated as M rises.This is seen in figure 3 and 4.

Figure 5. Illustrates way the behaviour of dimensionless temperature with the radiation parameter. Clearly, it is observed that the thermal boundary layer becomes thicker with escalating radiation factor. During the process of radiation, the flow liquid spawns a greater amount of heat; hence, both the temperature and thickness of the thermal layer are both augmented.

The effect of the exponential parameter N on flow parameters. It is observed from the Figure.6 that boost in N leads to a dwindling in flow field boundary layers. This occurs because the flow profiles exhibit a decreasing trend with increasing values of N. Particles moving away from the wall due to transmission of heat from the wall to the ambient fluid might be the cause of this occurrence, which can be explained by a decline in wall temperature through the boundary layer for N values.

The effect of exponential parameter has been depicted in Figure7 and 8. for smaller values of N, the trend increases suddenly and, at some point, starts to decrease gradually. But this is not the case for larger values of N. Contrariwise, for both larger and smaller values of N, the trend tends to decline. As N rises, $f'(\eta)$,$\theta(\eta)$ and $\phi(\eta)$ declines. Since the flow parameters are of exponential order, the value of N has a noticeable impact on the velocity field, temperature distribution and concentration distribution. Both for smaller and larger values of N, the novel results are procured.

It is seen in Figures 9,10 and 11 $f'(\eta)$,$\theta(\eta)$ and $\phi(\eta)$ declines as k gets magnified. Since every flow parameter has an exponential dependence on the flow field, the simultaneous effect of the exponential parameter and the chemical reaction parameter is significant.

A pictorial representation of the connection between the velocity graph and the heat source can be

seen in Figure 12 and 13 As can be seen in the graph, increases in Q_H values are accompanied by a drop in the velocity curves. The physical relationship between the heat source and the temperature is presented in Fig. The graph reveals that when Q_H values escalate, the curves exhibit decay, which is due to the heat source parameter releases the thermal energy to the flow, which causes increment of temperature profile. The impact of the Eckert number on the profile of temperature is disclosed in Figure 14. It is observed from the figure that an augmentation in Ec, the outcome of temperature is boosted. This enhancement happens because when work is done against the shear stress of the fluid motion, which produces kinetic energy into thermal energy i.e. dissipation of heat.

Portrays the velocity and temperature shape are influenced by the Casson parameter β in fig(15-16). The velocity profile dwindling out as the Casson parameter value upsurges. As increasing the Casson values strengthen the fluid internal structure, increasing in viscosity and decline in yield stress, which help the movement of fluid. We noticed for this resistance is accountable for appreciation of temperature as well. It is very significant to that for larger values of β leads to Newtonian fluid.

Absorption of electromagnetic radiation transforms electromagnetic energy into internal energy. This transformation generates heat, which in turn escalates the temperature distribution. Characteristic the consequencesof different values of R_a for various values of Prandtl number Pr= 6.83 (methanol) and Pr= 0.7 (air) is noted in Figure 17. In the case of larger values of Pr, i.e., for methanol(in this case), the curve slightly rises and close(near) to the wall and reduces smoothly apart from the wall. But this trend isvery far from wall for smaller values Pr,i.e., air. Thus, as R_a boosts up, temperature profile.

Effect of Joules heating parameter $Jh = 1, 2$ and 3 on Velocity, Temperature and Concentration profiles for fixed parameters $Ec = 0.1$, $R_a = 0.5$, $Gr = 1$, $Gc = 1$, $Pr = 0.7$, $Sc = 0.6$, $S = 0.5$, $N = 1$, $R = 0.3$, $Q_H = 0.4$, $\beta = 0.5$, $k = 0.1$ are disclosed in the figures(18-20). and the corresponding magnetic parameter values are obtained from the relation $Jh = M\,Ec$ .When an electric conducting fluid passing through a magnetic field ,part of the electro energy convert in to thermal energy., which in turn the enhance the temperature of the fluid as escalation the joule parameter values and opposite trend noticed in concentration and velocity profiles.

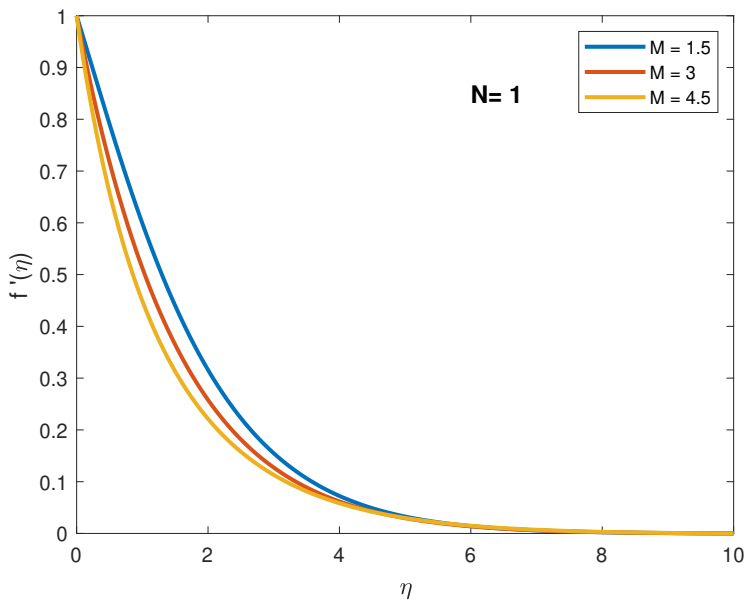

Figure 2: Velocity profile for various M

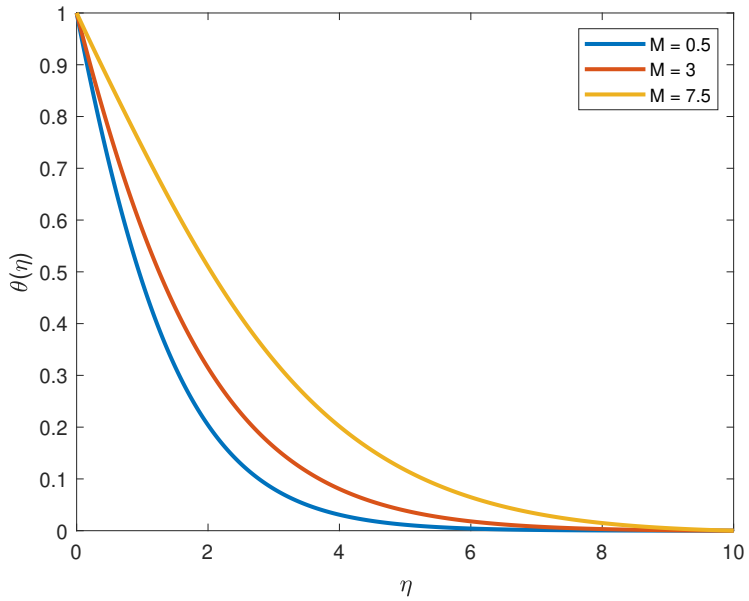

Figure 3: Temperature profile for various M

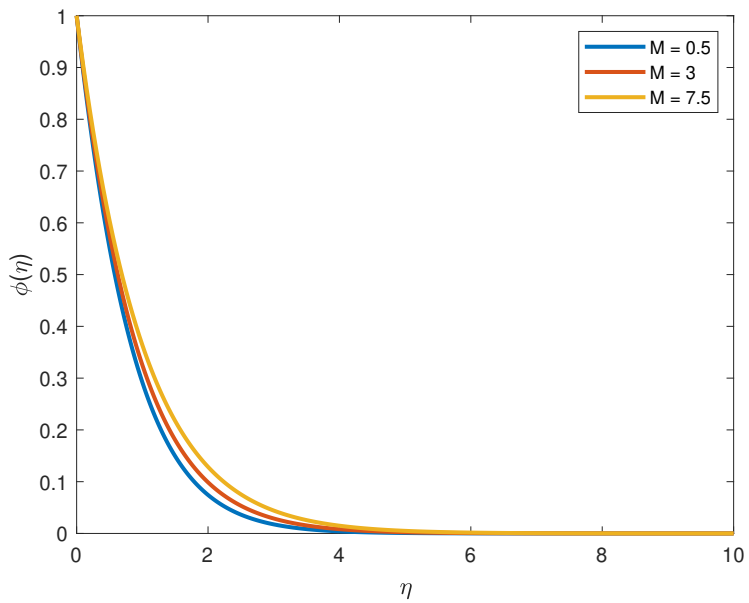

Figure 4: Concentration distribution for various M

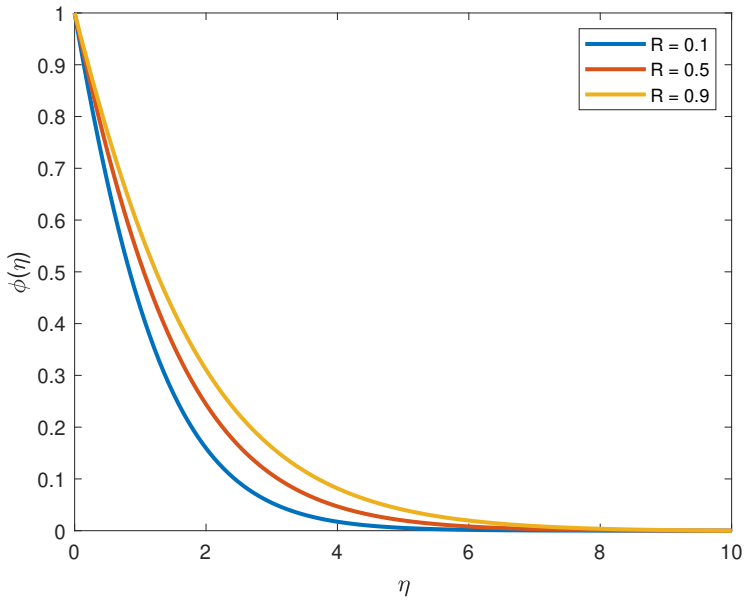

Figure 5: Temperature distribution for various R

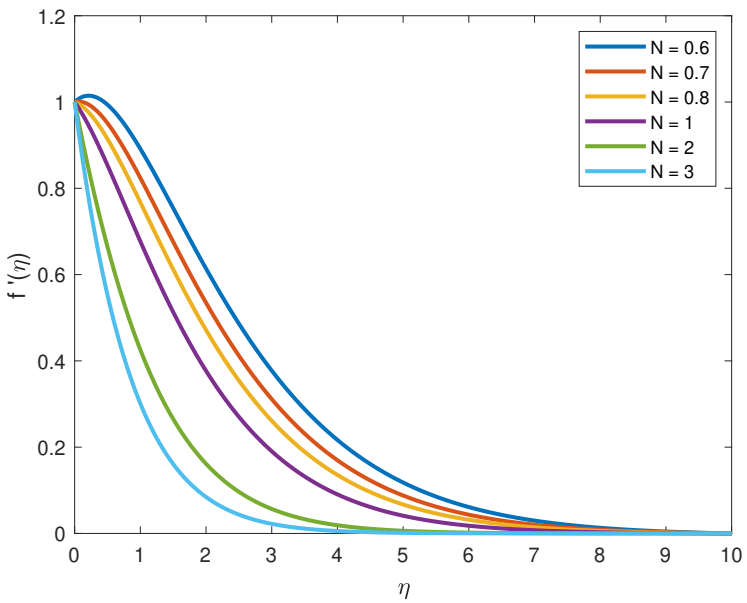

Figure 6: Velocity profile for various N

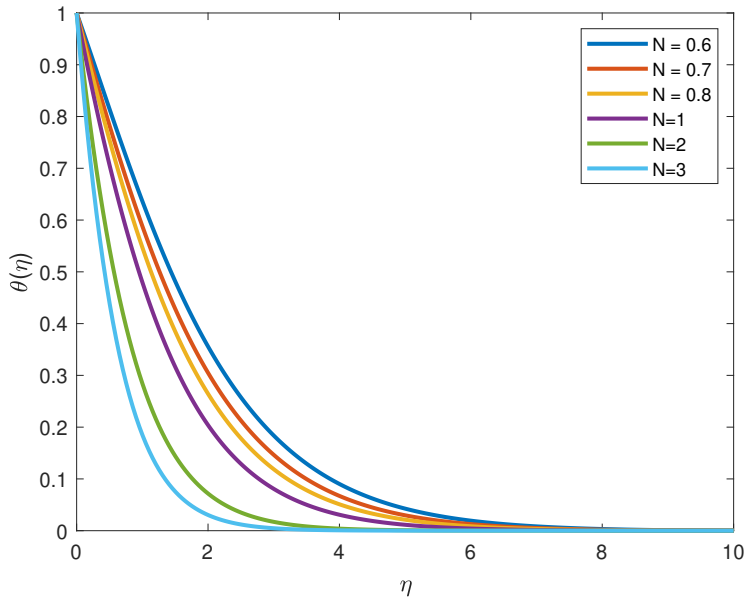

Figure 7: Temperature distribution for various N

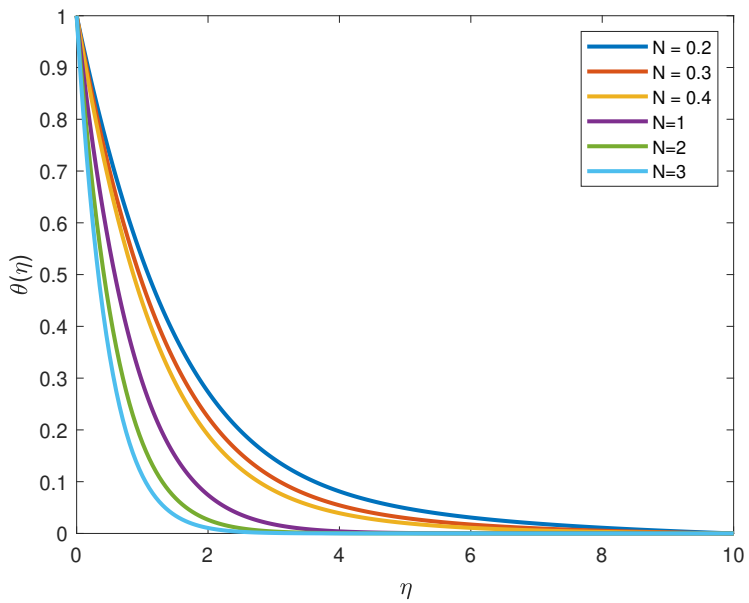

Figure 8: Concentration distribution for various N

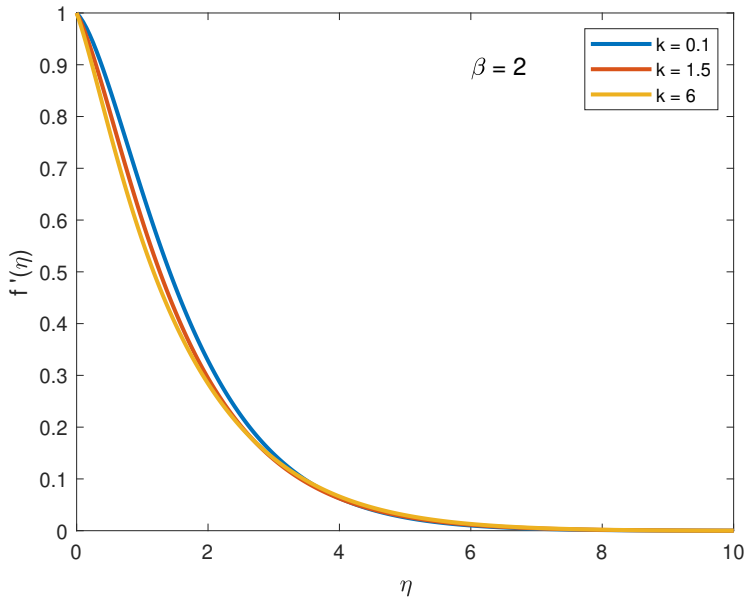

Figure 9: Velocity profile for various k

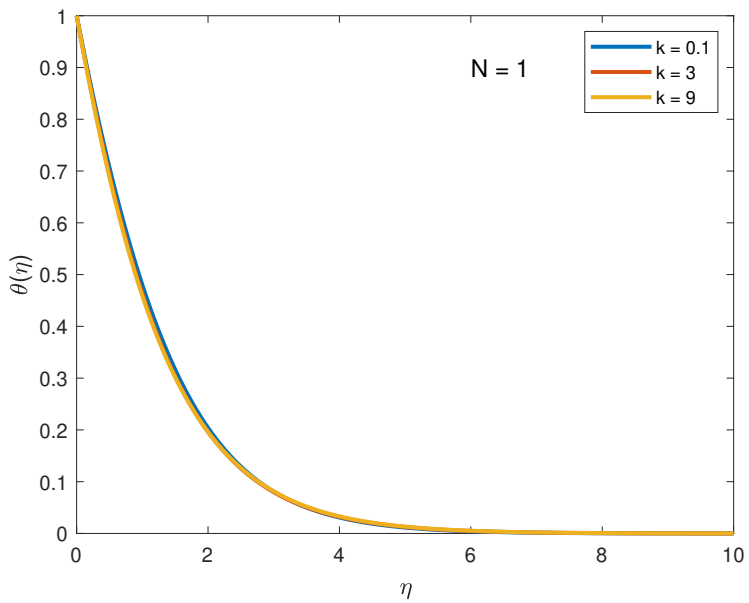

Figure 10: Temperature distribution for various k

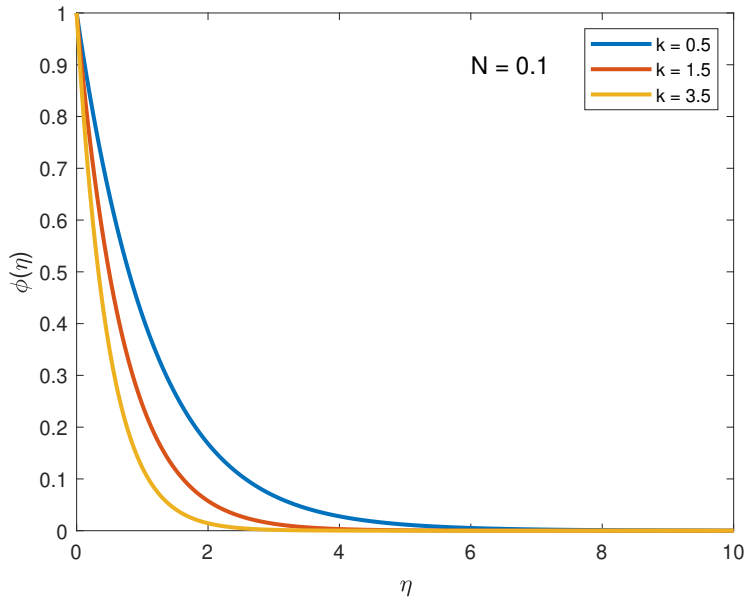

Figure 11: Concentration distribution for various k

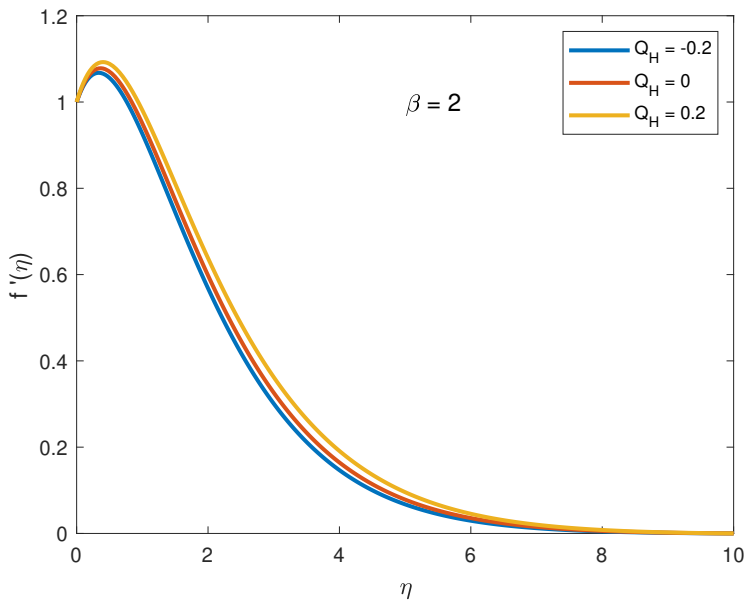

Figure 12: Velocity profile for various Q_H

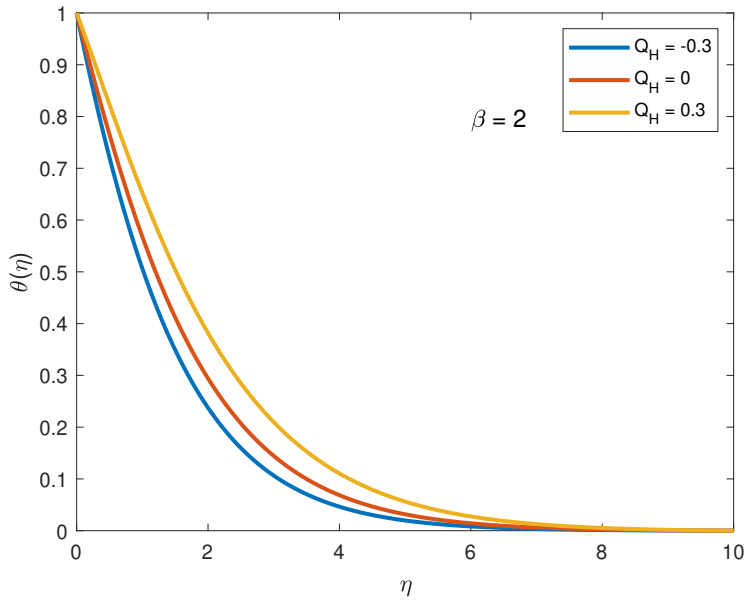

Figure 13: Temperature distribution for various Q_H

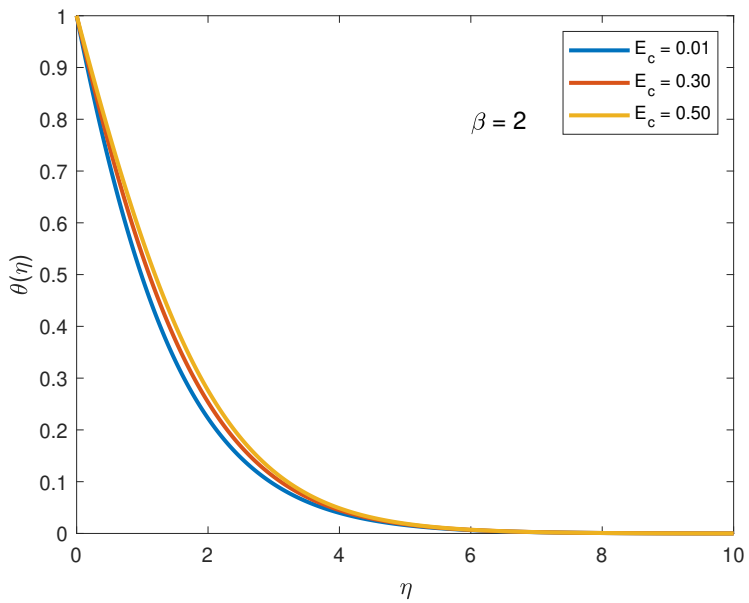

Figure 14: Temperature distribution for various E_c

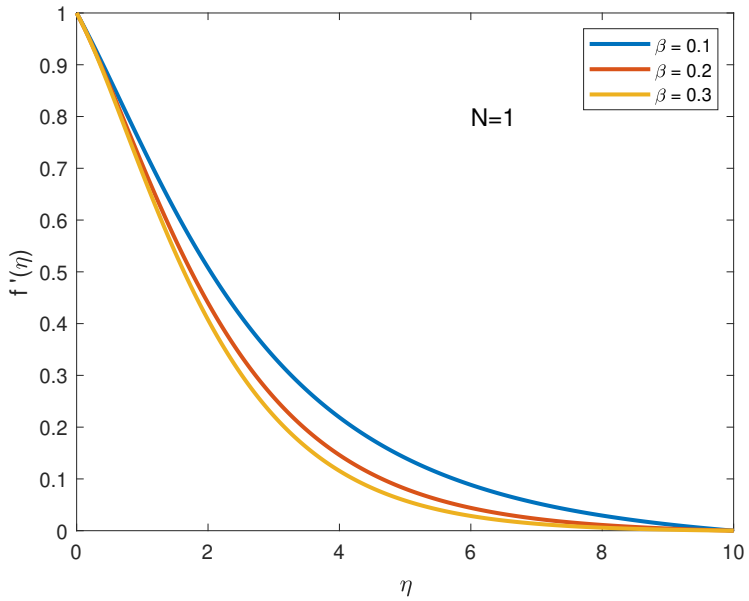

Figure 15: Velocity profiles for various β

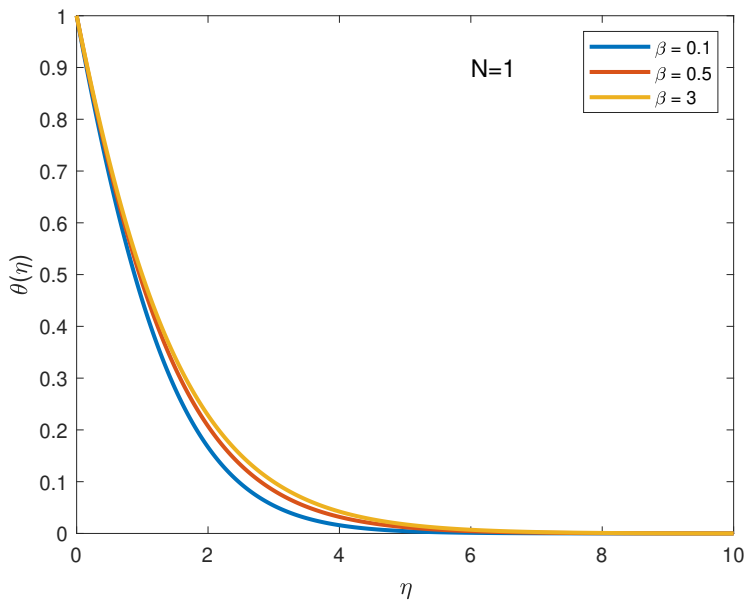

Figure 16: Temperature distribution for various β

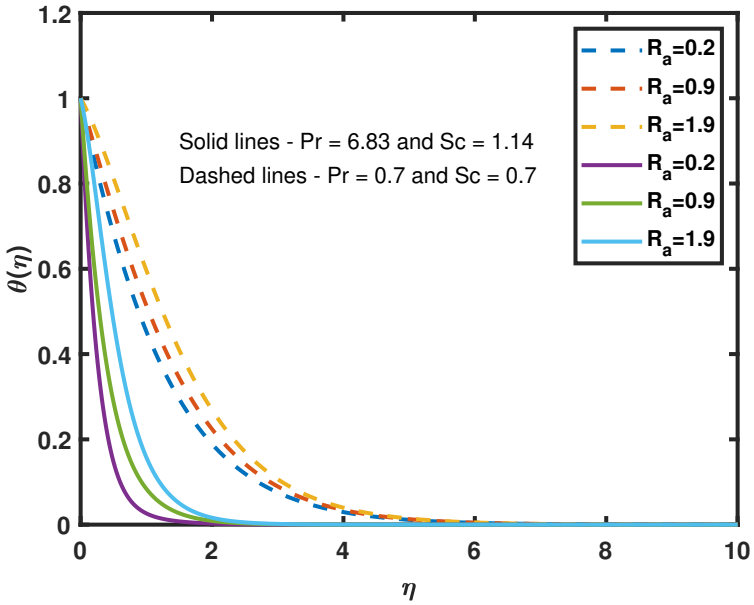

Figure 17: Temperature distribution for various R_a

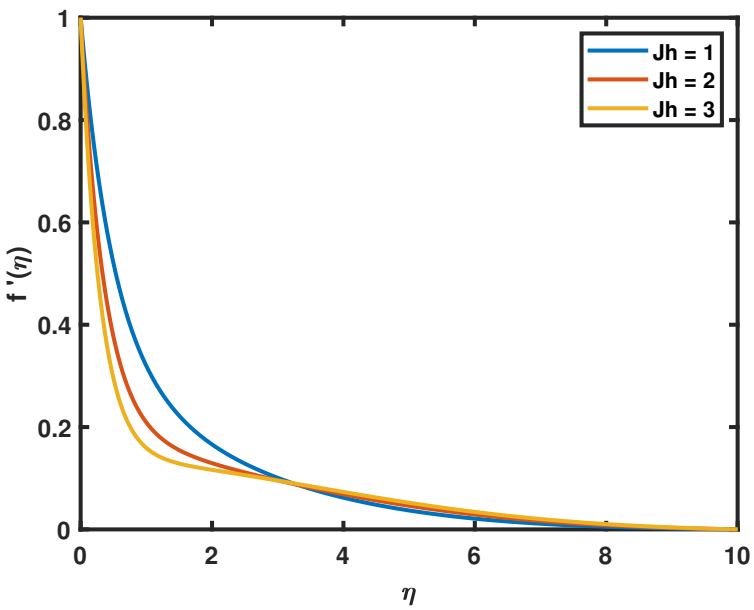

Figure 18: Effect of Joule heating parameter Jh on Velocity Profile

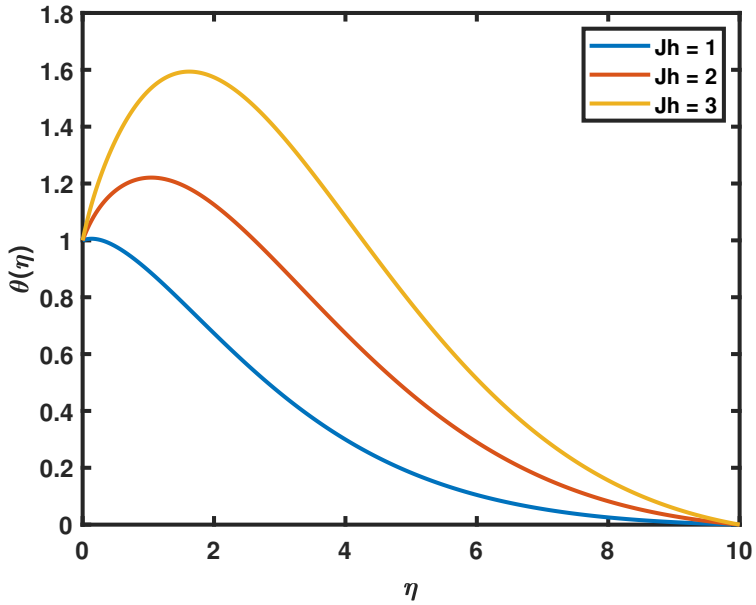

Figure 19: Effect of Joule heating parameter Jh on Temperature Profile

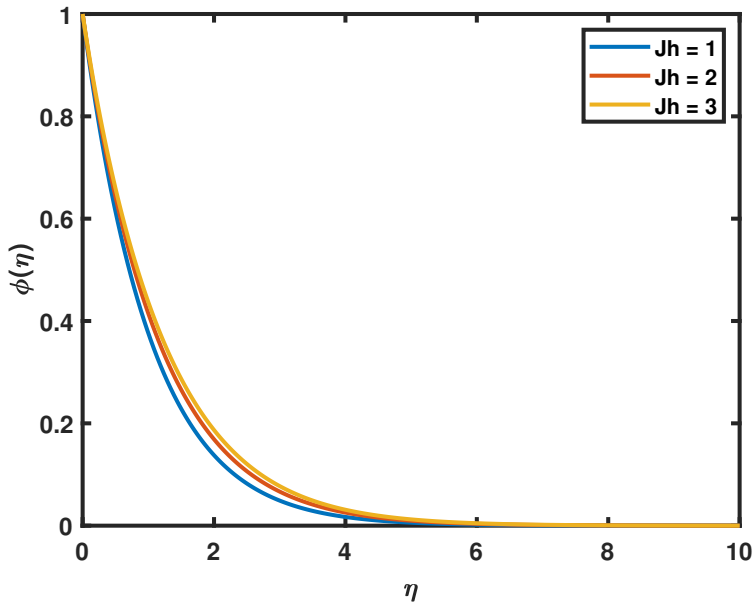

Figure 20: Effect of Joule heating parameter Jh on Concentration Profile

6. Conclusion

The outcomes the study briefly explained as follows: The increasing values of M upsurge the temperature & concentration, but opposite trend in velocity profile, which in turn the enhance the values of Sherwood and Nusselt. Temperature and thermal boundary layer are upsurges with the joule heating

and radiation absorption parameter.

It is noticed that the effect of stretching sheet N is very much influencing the velocity and demises the fluid movement.

It is also observed that the impact of Pr in the temperature profile is important ,for their impact on radiation absorption are significant

References

1. E. Magyari and B. Keller, *Heat and mass transfer in the boundary layers on an exponentially stretching continuous surface*, J. Phys. D: Appl. Phys. **32** (1999), 577–585.
2. P. S. Gupta and A. S. Gupta, *Heat and mass transfer on a stretching sheet with suction or blowing*, Can. J. Chem. Eng. **55** (1977), 744–746.
3. E. M. A. Elbashbeshy, *Heat transfer over an exponentially stretching continuous surface with suction*, Arch. Mech. **53** (2001), 643–651.
4. *A Textbook of Magnetohydrodynamics*, Pergamon Press, Oxford, 1965.
5. M. Q. Al-Odat, R. A. Damseh and T. A. Al-Azab, *Thermal boundary layer on an exponentially stretching continuous surface in the presence of magnetic field effect*, Int. J. Appl. Mech. Eng. **11** (2006), 289–299.
6. A. Ishak, *MHD boundary layer flow due to an exponentially stretching sheet with radiation effect*, Sains Malaysiana **40** (2011), 391–395.
7. I. C. Mandal and S. Mukhopadhyay, *Heat transfer analysis for fluid flow over an exponentially stretching porous sheet*, Ain Shams Eng. J. **4** (2013), 103–110.
8. N. Casson, *A flow equation for pigment-oil suspensions of the printing ink type*, Pergamon Press, New York.
9. S. Mukhopadhyay, K. Vajravelu and R. A. Van Gorder, *Casson fluid flow and heat transfer at an exponentially stretching permeable surface*, J. Appl. Mech. **80** (2013), 054502.
10. S. Pramanik, *Casson fluid flow and heat transfer past an exponentially porous stretching surface in presence of thermal radiation*, Ain Shams Eng. J. **5** (2014), 205–212.
11. M. Sajid and T. Hayat, *Influence of thermal radiation on the boundary layer flow due to an exponentially stretching sheet*, Int. Commun. Heat Mass Transfer **35** (2008), 347–356.
12. B. Bidin and R. Nazar, *Numerical solution of the boundary layer flow over an exponentially stretching sheet with thermal radiation*, Eur. J. Sci. Res. **33** (2009), 710–717.
13. F. S. Ibrahim, A. M. Elaiw and A. A. Bakr, *Effect of the chemical reaction and radiation absorption on unsteady MHD free convection flow*, Commun. Nonlinear Sci. Numer. Simul. **13** (2008), 1056–1066.
14. A. V. Kumar, D. Bhanumathi, S. V. Varma and Y. R. Yadav, *Effect of heat source, radiation absorption and chemical reaction on unsteady MHD flow*, Adv. Appl. Fluid Mech. (2013), 147–167.
15. G. Sreedevi, R. R. Raghavendra Rao, D. R. V. Prasada Rao and A. J. Chamkha, *Combined influence of radiation absorption and Hall current effects on MHD flow past a stretching sheet*, Ain Shams Eng. J. **7** (2016), 383–397.
16. N. N. Reddy, V. S. Rao and B. R. Reddy, *Chemical reaction impact on MHD natural convection flow past an exponentially stretching sheet*, Case Stud. Therm. Eng. **25** (2021), 100879.
17. M. Shamshuddin et al., *Thermo-solutal stratification and chemical reaction effects on radiative magnetized nanofluid flow*, J. Magn. Magn. Mater. **565** (2023), 170286.
18. M. Shamshuddin et al., *Unsteady thermo-solutal Brinkman electro-conductive nanofluid transport in rotating Hall MHD generator*, PDE Appl. Math. **7** (2023), 100525.
19. S. J. Reddy, P. Valsamy and D. S. Reddy, *Radiation and heat source effects on MHD Casson fluid flow over a stretching sheet*, J. Math. Comput. Sci. (2021).
20. Zeeshan et al., *Two-dimensional steady squeezing flow over a vertical porous channel*, Case Stud. Therm. Eng. **60** (2024), 104800.
21. M. Almheidat et al., *Entropy generation analysis of oscillatory magnetized flow with Joule heat over radiative sheet*, Case Stud. Therm. Eng. **61** (2024), 104921.
22. A. K. Sarma, *Magnetohydrodynamic flow with Soret and Dufour effects through a porous stretching plate*, Sigma J. Eng. Nat. Sci. (2025), 1533–1548.
23. A. Abbas et al., *Numerical simulation of MHD effects on heat generating Williamson Sakiadis flow with Joule heating*, Heliyon **9** (2023), e21726.
24. M. Sheikholeslami, H. R. Kataria and A. S. Mittal, *Radiation effects on heat transfer of three dimensional nanofluid flow*, Chin. J. Phys. **55** (2017), 2254–2272.

25. M. Shamshuddin et al., *Hall current, viscous and Joule heating effects on radiative MHD polymer dynamics*, Therm. Sci. Eng. Prog. **20** (2020), 100732.

26. C. Arruna Nandhini, S. Jothimani and A. J. Chamkha, *Radiation absorption and chemical reaction on Casson fluid over stretching sheet*, PDE Appl. Math. **8** (2023), 100534.

27. L. F. Shampine, J. Kierzenka and M. W. Reichelt, *Solving boundary value problems for ordinary differential equations in MATLAB with bvp4c*, (2000).

28. L. F. Shampine, I. Gladwell and S. Thompson, *Solving ODEs with MATLAB*, Cambridge University Press, 2003.

Kethoju Chandana,
Department of Mathematics, University College of Science,
Osmania University, Hyderabad, Telangana, 500007, India.
E-mail address: chandanakethoju@gmail.com

and

S.Hari Singh Naik,
Department of Mathematics, University College of Science,
Osmania University, Hyderabad, Telangana, 500007,India.
E-mail address: sharisinghnaik@osmania.ac.in

and

Ramesh Kune,
Sreenidhi Institute of Science and Technology,
Hyderabad, Telangana, India.
E-mail address: ramesh.k@sreenidhi.edu.in